Protist, 2007: 158, 365-383.

Morphological and molecular diversity of the monocercomonadid genera *Monocercomonas*, *Hexamastix* and *Honigbergiella* gen. nov

Hampl, V., Cepicka, I., Flegr, J., Tachezy, J., Kulda, J.

Morphological and molecular diversity of the monocercomonadid genera *Monocercomonas, Hexamastix* and *Honigbergiella* gen. nov.

Vladimír Hampl*, Ivan Cepicka, Jaroslav Flegr, Jan Tachezy and Jaroslav Kulda

Department of Parasitology, Faculty of Science, Charles University, Prague, Czech Republic

*Corresponding author: Vladimír Hampl, Department of Parasitology, Faculty of Science, Charles University in Prague, Vinicna 7, 128 44 Prague 2

Phone: +420 221951816

Fax: +420 224919704

E-mail: vlada@natur.cuni.cz

Running title: Diversity of monocercomonadids

Keywords: *Hexamastix*, *Honigbergiella, Monocercomonas,* morphology, phylogeny, ultrastructure.

ABSTRACT

Family Monocercomonadidae (Parabasala, Trichomonadida) is characterized by the absence of a costa and in most species also of an undulating membrane, both of which are typical structures of trichomonadids. We have examined 25 isolates of Monocercomonadidae species by sequencing of SSU rDNA and ITS region and by light and transmission electron microscopy. The isolates formed three distinct phylogenetically unrelated clades: 1) *Monocercomonas colubrorum*, 2) *Monocercomonas ruminantium* together with a strain ATCC 50321 designed as *Pseudotrichomonas keilini* and 3) *Hexamastix*. Twenty isolates of *Monocercomonas colubrorum* divided into three clades with no host-specificity. The morphological differences among clades were insufficient to classify them as a separate species. Non-monophyly of the cattle commensal *Monocercomonas ruminantium* with the type species *Monocercomonas colubrorum* and absence of *Pseudotrichomonas* characters in the free-living strain ATCC 50321 led to their reclassification into a new genus (*Honigbergiella* gen. nov.). The close relationship of these strains indicates a recent switch between a free-living habit and endobiosis. Two strains of *Hexamastix* represented different species – *Hexamastix kirbyi* Honigberg 1955 and *Hexamastix mitis* sp. nov. Polyphyly of Monocercomonadidae confirmed that the absence of costa and undulating membrane are not taxonomically significant characters and were probably secondarily lost in some or all clades. Our observations, however, indicated that other characters – infrakinetosomal body, comb-like structure, marginal lamella and the type of axostyle – are fully consistent with the position of Monocercomonadidae species in the parabasalian tree and are, therefore, reasonable taxonomic characters.

INTRODUCTION

Parabasalids are an abundant group of flagellates, mostly intestinal commensals of vertebrates and insects, whose common features include: the presence of hydrogenosomes (modified mitochondrion), a parabasal apparatus (Golgi body attached to a striated fibers), and nuclear division by a closed pleuromitosis with external spindle. The cell cycle of parabasalids typically includes only free-swimming trophozoites; true cysts are reported from a few species (Brugerolle 1973; Dolan *et al.* 2004; Farmer 1993).

In a simplified fashion, we can divide parabasalid species in two different types. 1) Ordinary flagellates with a single karyomastigont with up to five anterior flagella and one recurrent flagellum that typically forms an undulating membrane. The undulating membrane is usually underlain by a striated fiber – the costa. A tube-like microtubular sheet – the axostyle – forms the longitudinal axis of the cell. Its opened proximal end extends in a spoon-like capitulum that, together with an adjacent microtubular sheet (the pelta), partially surround the nucleus and perikinetosomal area. All these flagellates are classified into the order Trichomonadida. 2) The second type represents rather extravagant flagellates, whose mastigonts are, with the exception of devescovinids, multiplied and have group-specific organizations and distributions. In calonymphids the nuclei are also multiplied. All these species inhabit the intestines of insects and are classified into orders Cristamonadida, Trichonymphida and Spirotrichonymphida.

Based on morphological comparisons, it has been suggested that trichomonadids represent the ancestral morphology of parabasalids. The basal phylogenetic position in trichomonadids has been ascribed to organisms in the family Monocercomonadidae, the simplest trichomonadids, which lack an undulating membrane and costa. Their simple morphology was regarded as the relict of the cell organization of primitive parabasalids (Brugerolle 1976; Honigberg 1963). Molecular phylogenetic studies have cast doubt on this scenario of evolution by showing that monocercomonadids are polyphyletic, forming at least four groups in the tree, with none of them situated at the root (Dacks and Redfield 1998; Delgado-Viscogliosi *et al.* 2000; Edgcomb *et al.* 1998; Gerbod *et al.* 2000; Gerbod *et al.* 2001; Gerbod *et al.* 2002; Gerbod *et al.* 2004; Hampl *et al.* 2004; Keeling *et al.* 1998; Keeling 2002; Ohkuma *et al.* 2005). The polyphyly of monocercomonadids implies that the simple morphology of at least some monocercomonadid clades must have resulted from secondary reduction, unless we accept the independent origin of the undulating membrane and costa in

three trichomonadid clades (Hampl *et al.* 2004). On the other hand, the morphologically derived trichonymphids appeared at the root of parabasalids in analyses of SSU (small subunit) rRNA (Dacks and Redfield 1998; Delgado-Viscogliosi *et al.* 2000; Keeling *et al.* 1998; Ohkuma *et al.* 1998), GADPH, enolase and α-tubulin (Gerbod *et al.* 2004). Although the basal placement of trichonymphids in the SSU rRNA gene tree was doubted (Hampl *et al.* 2004), some protein phylogenies and most importantly the concatenation of α-, β-tubulin, enolase and GAPDH (Ohkuma *et al.* 2007) relatively strongly support its correctness.

As the result of unclear phylogenetic relationships, the taxonomy of parabasalids is in a state of flux. Previous division of parabasalids into two orders – Hypermastigida and Trichomonadida (Brugerolle 1976; Hollande and Caruette-Valentin 1971; Honigberg 1963) – has gradually been replaced by division into four orders – Trichomonadida, Cristamonadida, Trichonymphida and Spirotrichonymphida (Adl *et al.* 2005; Brugerolle and Patterson 2001). This is, however, also incongruent with current phylogenies, because the order Trichomonadida appears polyphyletic with order Cristamonadida and Spirotrichonymphida sitting inside it (e.g. Hampl *et al.* 2004; Hampl *et al.* 2006; Ohkuma *et al.* 2005; Noël *et al.* 2007). Noël *et al.* (2007) proposed a return to the two-order division by inclusion of cristamonadids and spirotrichonymphids as families within Trichomonadida. The classification inside the order Trichomonadida was lately revised by us (Hampl *et al.* 2006) by abolishing of family Cochlosomatidae and polyphyletic subfamilies within Trichomonadidae and by splitting the polyphyletic family Trichomonadidae into three monophyletic families – Trichomonadidae, Tritrichomonadidae and Trichomitidae. Last family of Trichomonadida, Monocercomonadidae, remained untouched although it is clearly untenable in the long term due to its polyphyletic nature.

The present paper does not aim to revise higher parabasalian classification but rather further explore parabasalian diversity. Here we present a morphological, ultrastructural and phylogenetic analysis of 25 isolates (12 newly reported) with monocercomonadid morphology formerly ascribed to genera *Monocercomonas*, *Hexamastix* and *Pseudotrichomonas*. Detailed inspection revealed important structural differences among superficially similar species, which correspond with their phylogenetic affiliation and together resulted in suggested nomenclature changes.

RESULTS

Phylogenetic position and relationship among isolates

Sequences of the SSU rDNA and the ITS region (ITS1, 5.8S rDNA, ITS2, and adjacent part of the LSU (large subunit) rDNA) were determined for all strains. Information on the accession numbers of the obtained sequences is given in the table 1.

A phylogenetic tree of parabasalids, based on the determined SSU rDNA sequences and available sequences from databases (fig. 1), was constructed by maximum likelihood methods and the statistical support was calculated by distance, maximum parsimony, maximum likelihood and Bayesian methods, respectively. The sequences of our isolates formed three well supported groups in the tree: 1) *Monocercomonas colubrorum* strains R183, R186, GRIS, PYR-1, LA10, R293, HYDR1, BOA1, BOA4, BOA5, MONT1, CHEL1, BIGA, EUMM, HAD, VAR-1, R208, TSC, CORON1. These isolates formed a robust clade together with the ATCC strain NS-1PRR. The clade was related to genera *Tritrichomonas*, *Dientamoeba*, *Histomonas*, and the orders Cristamonadida and Spirotrichonymphida. 2) *Monocercomonas ruminantium* strains HER-5 and KOJ-14 that were very closely related to the ATCC strain 50321 designated as *Pseudotrichomonas keilini*. 3) Two *Hexamastix* strains CYCL and T that formed a long branch related to termite symbionts ascribed to the genus *Tricercomitus*.

To further investigate the relationships within the *Monocercomonas colubrorum* clade, we also used for phylogenetic reconstruction the sequences of ITS region, which is more polymorphic. The tree in fig. 2 was constructed from the concatenated sequences of SSU rDNA and the ITS region using the same methods as for the whole parabasalian tree. The isolates split into three robust clades. The tree was rooted with the clade 1 (R183, R186 and GRIS) that appeared basal in the analysis with outgroups (not shown). The second clade consisted of isolates TSC, LA10, CORON1 and R293 and twelve remaining isolates formed the third clade together with the ATCC strain Ns-1PRR. Some sequences were identical (see zero branch lengths in fig. 2). Members of clades 1 and 2 differed by 54-62 nucleotides, members of clades 1 and 3 differed by 57-72 nucleotides and members of the clades 2 and 3 differed by 34-45 nucleotides in the concatenated sequences of SSU rDNA and the ITS region. For comparison, two morphologically well defined species *Trichomonas vaginalis* and *Trichomonas tenax* differed in the same region in 56 nucleotides. Relationships among isolates did not correspond to their host origin and none of the three clades was host-specific. In some cases, sequentially identical isolates colonized unrelated reptilian hosts, e.g. strains MONT1, CHEL1, EUMM, BIGA and PYR were isolated from chameleons, blue-tongue and two unrelated snakes, respectively.

Isolates of *Monocercomonas ruminantium* and *Hexamastix* are unrelated to the reptilian strains and, thus, were not included in the latter tree, but their genetic distances were also measured. *Monocercomonas ruminantium* strains HER5 and KOJ14 were identical in the concatenated sequences of SSU rDNA and ITS region and differed in 27 positions from the strain ATCC 50321 designed as *Pseudotrichomonas keilini*. The two *Hexamastix* strains differed in 101 nucleotides.

Morphology and ultrastructure of isolates

The cultured organisms were studied in fresh mounts using phase contrast microscopy, in fixed protargol stained preparations and using transmission electron microscopy. Their qualitative morphological characters are summarized in table 3.

Detailed examinations of strain ATCC 50321, deposited in ATCC as *Pseudotrichomonas keilini*, which is presented below, revealed that it does not possess morphological characters of the genus *Pseudotrichomonas*. Morphological similarity of this strain and the cattle strains HER5 and KOJ14 representing the species *Monocercomonas ruminantium* together with the phylogenetic positions of these three strains prompted their classification into a new genus *Honigbergiella* gen. nov.

Honigbergiella ruminantium n. comb. – strains HER5 and KOJ14

Motile trophozoites and round cysts were observed in cultures of strains HER5 and KOJ14. The protargol-stained specimens of strain HER5 (figs. 3A,B and 4A) essentially corresponded to the morphology of *Monocercomonas ruminantium* (Braune, 1913) Levine, 1961, as described by Jensen and Hammond (1964). They were typically ovoid or round in shape, the body, not including the axostyle, was 5.2±0.9 (3.7-7.8) μm long and 4.3±0.8 (2.9-6.2) μm wide, had three anterior flagella of slightly uneven lengths and one posterior flagellum, which neither formed an undulating membrane nor adhered to the body. An oval nucleus was 1.4±0.2 (0.9-2.1) μm long and 1.0±0.2 (0.5-1.5) μm wide. The parabasal body was disc-shaped, and typically situated on the latero-anterior part of the nucleus. The slender axostyle originated at the anterior pole of the cell, extended through the longitudinal axis of the cell, and protruded posteriorly. The length of the free portion of axostyle varied from 10 to 100 % (average 45%±20%) of the cell length. Anteriorly, the axostyle formed a narrow capitulum. The pelta was relatively small. Parabasal fibers stained very weakly.

The ultrastructure of trophozoites of strain HER5 (fig. 5) was similar to that of other trichomonads. Four basal bodies were situated at the anterior pole of the cell. The basal body

of the recurrent flagellum was positioned orthogonally to the basal bodies of the anterior flagella. The recurrent flagellum did not adhere to the cell, did not form an undulating membrane and the marginal lamella was absent. A costa was also absent. The Golgi body was situated anteriorly to the nucleus and was connected to basal body 2 by a striated parabasal fiber (PF2). Both the infrakinetosomal body and the comb-like structure were absent. A microtubular axostyle overlapped near the basal bodies with microtubules of the pelta, which underlay the most anterior part of the cell. The cytoplasm contained food vacuoles, hydrogenosomes and numerous glycogen granules. The cysts of strain HER5 were spherical, with a cyst wall separated from the plasma membrane and coated by a glycocalyx. The cytoplasm of the cysts was more granular than that of trophozoites and contained the nucleus, hydrogenosomes and internalized flagella.

Honigbergiella sp. strain ATCC 50321

The strain ATCC 50321 was deposited in ATCC as *Pseudotrichomonas keilini*, but it does not possess an important character of the genus – the undulating membrane (figs. 3C, D and 6). It shares all characters of *Honigbergiella* as described above. As the phylogenetic analyses revealed its close relationship with strains HER5 and KOJ14, there is no doubt that these organisms are congeneric. Strain ATCC 50321 formed true cysts like the strains HER5 and KOJ14 but failed to grow at 37 °C. Protargol-stained trophozoites (fig. 3C, D and 4B) were identical in all qualitative characters to the previous strains and only slight differences were observed in dimensions. The cell body, not including the axostyle, was 5.5±0.8 (3.8-7.2) μm long and 4.5±0.9 (3.1-7.2) μm wide, which was on average slightly larger than HER5, but the difference was not statistically significant. The nucleus was also larger, 1.7±0.3 (1.1-2.5) μm long and 1.1±0.2 (0.6-1.6) μm wide, and these differences were statistically significant ($p<0.001$, N=50). The length of the extracellular part of axostyle varied from 10 % to 60 % of the cell length (average 25%±10%), which is significantly less ($p<0.001$, N=50) than in *Honigbergiella* strain HER5. No difference in the free axostyle length was observed in living cells using phase contrast microscopy.

Monocercomonas colubrorum strains

Motile trophozoites and pseudocysts with internalized flagella were observed in cultures of the reptile strains R-183, R186, GRIS, TSC, LA10, R293, CORON1, NS-1PRR, R-208, PYR 1-1, EUMM, BIGA, MONT1, CHEL1, HAD, HYDR1, VAR, BOA1, BOA4 and BOA5. Strains R183, R186, TSC, LA10, R293, NS-1PRR, EUMM, HAD, HYDR1 and BOA5 were

stained with protargol and representatives of each clade and the strain NS-1PRR, which formed a long branch in the tree, are given in fig. 7. Their morphology was very similar and corresponded to *Monocercomonas colubrorum*. Trophozoites had an oblong shape, three anterior flagella of slightly unequal length and one posterior flagellum. Undulating membranes and costa were not developed, the adherent proximal part of the posterior flagellum trailed above the nucleus in the posterior-right direction. The axostyle was relatively stout. It protruded from the cell posteriorly and gradually narrowed to the tip. Anteriorly, the axostyle formed a spoon-like capitulum covering the nucleus. The pelta formed a scoop-like structure supporting the anterior protrusion of the cell. The parabasal body had the shape of a rod and was situated on the right anterior edge of the nucleus, typically under the proximal part of the recurrent flagellum.

The strains differed in the dimensions of the cell, nucleus and the relative length of the free part of the axostyle (table 2). Some differences were statistically significant, but, generally, did not correspond with the phylogenetic relationship of strains. For some parameters (cell and nucleus length and width), the variability within clades was higher than among clades and the result of multivariate cluster analysis based on the cell dimensions also failed to correspond to their phylogeny (not shown). However, three characters corresponded to the distribution of strains in clades. The cell length-to-width ratio is the smallest in clade 2 and the pool of values of the clade 2 strains differed significantly from the pool of values of the clade 1 strains as well as the clade 3 strains ($p<0.001$). The difference between clades 1 and 3 was not significant. Analogously the relative length of the axostyle protrusion was significantly higher in the clade 1 than in the clades 2 or 3 ($p<0.001$). Finally, we observed a difference in the shape of axostyle capitulum, which was wider in clade 2 than in the other two clades.

Strains also differed in the capability of phagocytosis. Strains TSC and R293 from the clade 2 massively phagocytized starch granules and bacteria, while trophozoites with engulfed bacteria or starch were observed only rarely in the other two strains from clade 2 and any strain from clades 1 and 3.

Strain VAR-1 was examined by the electron microscope (fig. 8). Its internal structure was essentially identical to that of strain NS-1PRR examined by Mattern *et al.*. (1972). The mastigont consisted of three anterior and one recurrent basal body, infrakinetosomal body, pelta-axostylar complex and several striated fibers including a comb-like structure. The recurrent flagellum did not form an undulating membrane and was in its proximal part underlain by the marginal lamella. A costa was absent. The Golgi body was situated latero-

anteriorly from the nucleus and was connected to the basal bodies by the striated parabasal fiber (PF2). The axostyle formed a broad capitulum, sigmoid fibers (F2) connected basal body 2 with the pelta at the pelta-axostylar junction. Pseudocysts (fig. 8C) were enveloped by uncovered plasma membrane and an internalized karyomastigont and internalized flagella were observed inside pseudocysts.

Hexamastix mitis spec. nov. strain CYCL

In the culture of the strain CYCL, we observed only trophozoites; neither cysts nor pseudocysts were present. The morphology of the protargol-stained specimens (figs. 9A-D and 10A,B) did not correspond to any described species, from which it differed by possessing a large disc-shaped parabasal body with a central granule, and a slender axostyle. Trophozoites had round or ovoid cells, the body (axostyle not included) was 7.8±1.1 (5.8-11.3) μm long and 7.1±1.1 (5.3-11.2) μm wide, had six flagella of uneven lengths and an oval nucleus 2.4±0.3 (1.6-3.2) μm long and 1.6±0.2 (1.1-2.1) μm wide. Neither an undulating membrane nor a costa were developed. The extracellular part of the axostyle was not observed in many specimens and if observed was relatively short, extending on average 20%±10% (10%-50%) of the cell length. The capitulum of the axostyle was narrow. and the pelta was relatively small.

Hexamastix kirbyi strain T

In the culture of the strain T, we observed only trophozoites, neither cysts nor pseudocysts were present. The morphology of protargol-stained specimens (figs. 9E-F and 10C, D) corresponded to *Hexamastix kirbyi* Honigberg, 1955. Trophozoites were ovoid, oval or round in shape, the body without axostyle was 7.7±1.0 (6.1-9.9) μm long and 6.0±0.9 (4.2-8.5) μm wide. Cells had six flagella of uneven length and an oval nucleus 2.1±0.3 (1.4-2.9) μm long and 1.3±0.2 (0.9-1.9) μm wide. Undulating membranes and costa were not developed. The axostyle was slender, expanding abruptly into a broad capitulum in the nuclear area. Its distal part stretched out 30%±10%(10%-50%) of the cell length. The pelta was relatively large. The parabasal body had a shape of a small ring or a tear with a dark stained outline and was situated at the anterior part of the nucleus or above the nucleus close to the basal bodies. Parabasal fibers were not visible by light microscopy.

The ultrastructure of strain T (fig. 11) corresponded to that of *Hexamastix* in Brugerolle (1976). The basal body of the recurrent flagellum was positioned orthogonally to the five basal bodies of anterior flagella. Basal body 2 bore the parabasal fibers (PF) and the

sigmoid fibers (F2) directed to the pelta-axostylar junction. Basal bodies 1 and 3 bore hooked laminae F1 and F3. The Golgi body, associated with the parabasal fibers (PF2), was situated anterolaterally to the nucleus. A comb-like structure, infrakinetosomal body and marginal lamella were not present.

DISCUSSION

Our isolates formed three distinct and unrelated clades in the parabasalian tree. The most species-rich clade was formed by the *Monocercomonas* isolates from reptiles. The taxonomy of the reptile species of *Monocercomonas* is rather confusing (see discussion in Honigberg (1963)). Up to 30 species were described, but descriptions are mostly insufficient and based on the assumed host specificity. Moskowitz (1951) and Honigberg (1963) recognized only two valid species, *Monocercomonas colubrorum* (Hammerschmidt, 1844) Doflein, 1901 and *Monocercomonas moskowitzi* Honigberg, 1963. The morphology of our strains corresponded with the description of *Monocercomonas colubrorum* by Moskowitz (1951) and differed from *Monocercomonas moskowitzi* in their longer cells, shorter adherent part of recurrent flagellum and the shape of axostyle, which had a longer external part that narrowed continuously to the tip, not abruptly as in *Monocercomonas moskowitzi*. The clade of *Monocercomonas colubrorum* appeared in our tree as a sister to a large clade of cristamonads, spirotrichonymphids and tritrichomonads, although the statistical support for such a position was low. The morphology of *Monocercomonas* can hardly be directly compared with spirotrichonymphids or cristamonadids, whose cell morphology is rather derived, probably as a result of accelerated evolution triggered by the selection pressure in the insect gut environment. However, *Monocercomonas* shares several characters with *Tritrichomonas*: the rigid shape of the cell, a stout tube-like axostyle, rod shaped parabasal body, and the presence of marginal lamella, comb-like structure and infrakinetosomal body (Mattern *et al.* 1972).

In the analyses based on concatenated sequences of SSU rDNA and the ITS region, strains of *Monocercomonas colubrorum* split into three robust clades. The nucleotide differences among the clades were higher or similar to the difference between the two valid species *Trichomonas vaginalis* and *Trichomonas tenax*. Distribution of strains in clades corresponded neither to their capability for phagocytosis nor to host taxon. Protargol-stained specimens of different strains exhibited differences in their morphology, but only two of these parameters, cell length-to-width ratio and relative length of axostyle protrusion, seemed to be

clade specific. These characters could, however, be affected by culture conditions and fixation. The only qualitative character that was potentially clade-specific was the shape of the axostyle capitulum, which was wider in clade 2. Although genetic distances suggested that the three clades might represent separate species, we did not find any firm diagnostic characters for these species and, therefore, for the present regard all examined strains as belonging to a single species, *Monoceromonas colubrorum*.

The only species, described from cattle, that possesses three anterior flagella and a free recurrent flagellum is *Monocercomonas ruminantium* (Braune, 1913) Levine, 1961. The strain HER5 shared most morphological characteristics with *Monocercomonas ruminantium* as described by Jensen and Hammond (1964) – size and shape of the cell, slender axostyle, disc-shaped parabasal body and formation of true cysts. It differs in the relative length of the extracellular part of axostyle, which was longer in our isolate. This difference could be ascribed to the fixation conditions and to the fact that Jensen and Hammond (1964) prepared smears directly from the hosts, while we stained specimens from culture. As the essential characters of the strain HER5 agreed with the description, we assume that HER5 and KOJ14 (whose sequence was identical to HER5) correspond to the species described by Jensen and Hammond (1964) as *Monocercomonas ruminantium*. In the phylogenetic tree, these strains did not form a clade with isolates from reptiles representing *Monocercomonas colubrorum*, the type species of the genus *Monocercomonas*, but branched inside the free-living-trichomonad clade close to ATCC isolate 50321. Generic classification of *Monocercomonas ruminantium* is thus not valid and is revised here. The affinity of strains HER5 and KOJ14 to the free-living species and Trichomonadidae *sensu* Hampl *et al.* (2006), corresponded with their morphology and ultrastructure – slender axostyle, smaller cells with less rigid shape and the absence of a comb-like structure and infrakinetosomal body.

The characteristic feature of the genus *Pseudotrichomonas* is the presence of a lamelliform undulating membrane (Brugerolle, 1991). We showed clearly that no undulating membrane is present in the isolate ATCC 50321, so the original identification of this isolate as *Pseudotrichomonas keilini* was incorrect. The morphology of this isolate closely resembled that of isolate HER5. The only difference that we detected was the relative length of the extracellular part of the axostyle and the size of the nucleus in fixed specimens. These differences can, however, be ascribed to variations in fixation conditions. Isolates HER5, KOJ14 and ATCC 50321 formed true cysts but unlike HER5 and KOJ14, ATCC 50321 failed to grow at 37°C. Morphological similarities between the isolates HER5 and ATCC 50321 corresponded to the very high similarity in their SSU rDNA and ITS region sequences. They

differed in 27 nucleotides (2 % divergence), which is certainly within the range of intrageneric differences in parabasalids.

Based on our findings, we establish a new parabasalid genus, *Honigbergiella* gen. nov., that harbors strain ATCC 50321 and the species formerly classified as *Monocercomonas ruminantium*. Strain ATCC 50321 differs from *Monocercomonas ruminantium* only slightly in morphology and sequence. However, because they differ also in ecology – free-living versus intestinal commensal - and in temperature tolerance, and because we consider these ecological characters significant, we keep them as separate species, *Honigbergiella* sp. and *Honigbergiella ruminantium*, respectively. The species status of *Honigbergiella* sp. needs to be resolved in the future.

The position of the commensal species *Honigbergiella ruminantium* in the clade of free-living species and its remarkable similarities to *Honigbergiella* sp. indicate that *Honigbergiella ruminantium* probably switched very recently from a free-living to a commensal way of life. An alternative explanation for this pattern would be two independent switches to a free-living habit in *Honigbergiella* sp. and the ancestor of *Ditrichomonas honigbergii* and *Monotrichomonas carabina*. This alternative, however, we regard as less probable. On the other hand, it cannot be excluded that *Honigbergiella* sp. was isolated from a creek that was contaminated by cattle feces and that *Honigbergiella* sp. is in fact a commensal able to survive for certain period in the fresh water. The true cysts with cyst wall, which we reported for both species, would make survival in harsh external conditions easier.

The sequences of the two *Hexamastix* isolates differed in approximately two times as many nucleotides as differed the species *Trichomonas vaginalis* and *Trichomonas tenax* indicating that these isolates very probably represent two distinct species.
The morphology of isolate T corresponded to the description of *Hexamastix kirbyi* in every essential detail (ring-shaped parabasal body, slender axostyle, the cell dimensions, relatively large pelta). The second isolate, CYCL, differed with the combination of a slender axostyle and a large disc-shaped parabasal body with central granule from all described species – *Hexamastix caviae* and *Hexamastix termitis* (stout axostyle), *Hexamastix batrachorum* (biarmed parabasal body), *Hexamastix crassus* and *Hexamastix robustus* (twisted axostyle) (Nie, 1950; Honigberg and Christian, 1954; Honigberg, 1955). We regard the isolate CYCL as a new species, *Hexamastix mitis* sp. nov.

In our analysis, the *Hexamastix* strains formed a long branch with a poorly supported position. The most probable sister clade to *Hexamastix* are the three termite symbionts ascribed to genus *Tricercomitus*. In fig. 1 *Hexamastix* and *Tricercomitus* branch together with

Trichonymphida. However, we have shown previously (Hampl *et al.* 2004) that this position is probably a result of long branch attraction (Felsenstein 1978) and the most probable position of *Hexamastix* and *Tricercomitus* is next to the clade of *Ditrichomonas*, *Monotrichomonas* and *Honigbergiella*. This position would correspond also to *Hexamastix* morphology – non-rigid cell shape and slender axostyle, in contrast to tube-like stout axostyle and rigid oblong shape of tritrichomonadids and *Monocercomonas colubrorum*. *Hexamastix* also does not possess a comb-like structure, infrakinetosomal body and marginal lamella. The position of the *Hexamastix* clade should be confirmed in the future using another gene.

The polyphyletic nature of family Monocercomonadidae, which results from our analyses, has been pointed out many times (Delgado-Viscogliosi *et al.* 2000; Dacks and Redfield 1998; Edgcomb *et al.* 1998; Gerbod *et al.* 2000; Gerbod *et al.* 2001; Gerbod *et al.* 2002; Gerbod *et al.* 2004; Hampl *et al.* 2004; Keeling *et al.* 1998; Keeling 2002; Ohkuma *et al.* 2005). The present study, however, shows that characteristics of species, other than the absence of costa and undulating membrane, correspond well with their position in the tree. These include the shape of axostyle and parabasal body, rigidity of the cell and the presence or absence of an infrakinetosomal body, comb-like structure and marginal lamella. Molecular phylogeny is, therefore, not in conflict with the morphology but only with the classification, which has been in this case based on non-relevant characters.

TAXONOMIC SUMMARY

Honigbergiella gen. nov. Hampl, Cepicka and Kulda

Diagnosis – Three anterior and one recurrent flagellum. Recurrent flagellum is not distinctly longer than anterior flagella. Undulating membrane, costa, marginal lamella, infrakinetosomal body and comb-like structure absent. Axostyle slender. Parabasal body disc-shaped. Production of true cysts. Free-living and endobiotic.

Type species – *Honigbergiella ruminantium* n. comb.
Etymology – Named after outstanding protozoologist Bronislaw M. Honigberg.

Hexamastix mitis spec. nov. Hampl, Cepicka and Kulda

Diagnosis – Body (without axostyle) 7.8±1.1 (5.8-11.3) μm long and 7.1±1.1 (5.3-11.2) μm wide, six flagella of uneven lengths, oval nucleus 2.4±0.3 (1.6-3.2) μm long and 1.6±0.2 (1.1-2.1) μm wide, parabasal body disc-shaped, axostyle slender with relatively short protruding part extending on average 20%±10% (10%-50%) of the cell length, capitulum of axostyle narrow, pelta relatively small.

Type host – *Cyclura nubila*.

Habitat – Isolated from feces. Presumably lives in the lower intestine.

Type locality – Prague, Czech Republic. The type host species naturally occurs in Cuba.

Syntype slides – Protargol preparations of the isolate CYCL, deposited in the collection of the Department of Parasitology, Faculty of Science, Charles University, Prague, Czech Republic.

Etymology – *mitis* [Latin] – fine, gentle, mild, soft. The axostyle and pelta of this species are small and fine.

MATERIAL AND METHODS

Organisms

Information on the origin of strains included in this study is summarized in table 1. All organisms, except strain CYCL, are deposited in the culture collection of the Department of Parasitology, Charles University in Prague, Czech Republic and are available upon request. Strain CYCL was not cultivable long term.

Cultivation

Reptile strains R-183, R186, GRIS, TSC, LA10, R293, CORON1, NS-1PRR, R-208, PYR 1, EUMM, BIGA, MONT1, CHEL1, HAD, HYDR1, BOA5, VAR1, BOA1 and BOA4 were maintained as axenic cultures in TYM medium (Clark and Diamond, 2002) supplemented with 10% heat-inactivated horse serum. The pH of the medium was adjusted to 7.2. Strains HER-5, KOJ-14, CYCL and T were maintained as xenic cultures with admixed bacteria in modified TYSGM-9 medium without mucin and tween, and with rice starch (Clark and Diamond, 2002). The strains HER-5, KOJ-14 were cultivated at 37^{o}C and the other strains, mostly reptilian isolates, at 26^{o}C. The cultures maintained in TYM were grown three transfers before harvesting in a medium without agar.

Light microscopy

Moist fixed films spread on cover slips were prepared from soft pellets of protists obtained by centrifugation (500G) of cultures. The films were fixed in Bouin-Hollande's fluid and stained with protargol (Bayer, I. G. Farbenindustrie Actinengesellschaft, Germany) according to the protocol recommended by Nie (1950). Trichomonads were observed and photographed with an Olympus BX51 microscope using immersion objective 100x UPPlanApo. Fifty specimens of each strain were measured from digital photographs using the Grmeasure software calibrated with objective micrometer. Only non-dividing cells stretched in horizontal plane were measured.

Statistical tests

The significance of differences in cell dimensions among strains was tested using ANOVA and post hoc test Scheffé in Statistica (StatSoft). Multivariate cluster analysis was also performed in Statistica (StatSoft).

Transmission electron microscopy

Pellets of protists, obtained by centrifugation (500G) of cultures, were fixed in 2.5% (w/v) glutaraldehyde and 5 mM $CaCl_2$ in 0.1 M Na-cacodylate buffer (pH 7.2) at room temperature for 2 hours. After washing three times in PBS, the cells were postfixed in 1% (w/v) osmium tetroxide, 0,8% potassium ferricyanide, and 5 mM $CaCl_2$ in 0.1 M Na-cacodylate buffer. After wash in excess of PBS, the fixed samples were dehydrated in an ethanol series, transferred to acetone, and embedded in Epon. Ultrathin sections were stained with uranyl acetate and lead citrate and examined with a Phillips EM 420 electron microscope.

PCR amplification

DNA was isolated using a High pure PCR template preparation kit, Roche (Indianapolis, USA). The 5.8S rRNA gene with the flanking areas ITS1 and ITS2 was amplified by PCR using trichomonad-specific primers designed according to the TFR1 and TFR2 primers described by Felleisen (1997); forward primer – ITSF (TTCAGTTCAGCGGGTCTTCC), reverse primer ITSR (GTAGGTGAACCTGCCGTTGG). The reaction mixture consisted of 75 mM Tris-HCl pH 8.8, 20 mM $(NH_4)_2SO_4$, 0.01 % Tween 20, 2.5 mM $MgCl_2$, 0.04 mM each dNTP, 0.001 mM both primers, 0.05 U/µl Taq polymerase and 0.5-5 ng/µl DNA. The reaction conditions were as follows: 39 cycles of 90^{o}C (0.5 min), 66^{o}C (0.5 min), 72^{o}C (1.5 min) ended by final extension step 72^{o}C (15 min.).

The SSU rDNA was amplified using trichomonad-specific primers 16Sl (TACTTGGTTGATCCTGCC) and 16Sr (TCACCTACCGTTACCTTG) (Tachezy *et al.* 2002). Reaction mixture consisted of 75 mM Tris-HCl pH 8.8, 20 mM $(NH_4)_2SO_4$, 0.01% Tween 20, 1.9 mM $MgCl_2$, 0.1 mM each dNTP, 0.25 µM both primers, 0.05 U/µl Taq

polymerase and 0.5-5 ng/µl DNA. The thermal cycle used was as follows: 92°C (4 min) for initial denaturation followed by 31 cycles of 94°C (1 min), 62°C (1 min), 72°C (2.5 min) and ended by a final extension step 72°C (10 min). In cases of isolates HYDR1 and CORON1, the annealing temperature was 57 °C.

In some cases, the whole region of SSU rDNA, 5.8S rDNA, ITS1 and ITS2 was amplified with primers 16Sl and ITSF. The composition of reaction mixture and the reaction conditions were identical as in the case of SSU rDNA.

Sequencing

The genes were mostly sequenced directly from PCR products. To confirm that the sequencing reaction from PCR product was not affected by presence of contaminating PCR products, PCR products of the xenic strains T, CYCL and KOJ-14 were also cloned to pGEM®-T Easy Vector using the pGEM®-T EASY VECTOR SYSTEM I (Promega) and sequenced from vector. For the same reason the PCR products of two axenic reptile isolates (PYR1-1 and TSC) were cloned and sequenced from vector. The directly determined sequence of xenic strain HER5 was identical to the sequence of KOJ14, so it was not cloned.

The external primers used for sequencing from vector were SP6 and T7.The external primers used for direct sequencing from PCR product were ITSF, ITSR, 16Sl and 16Sr. The primers used for sequencing of internal regions were 514F (GTGCCAGCMGCCGCGG), 665F (GTGAACAAATCAGGACGC), 1055F (GGTGGTGCATGGCCG), 1385R (GATCCTAACATTGTAGC), 1238R (TAATTGGYGATAATCTC), 1055R (CGGCCATGCACCACC), 665R (ATACWCTAAGCGTCCTG) and 295R (AGTCCGACGGTAACCGC).

The sequencing was carried out in an automatic genetic analyzer ABI PRISM 310 (PE Biosystems). Sequencing reaction was performed using the DNA Sequencing Kit, BigDye™ Terminator Cycle Sequencing (PE Biosystems).

Phylogenetic analyses

Alignment based on the secondary structure of SSU rRNA sequences of parabasalids was downloaded from the rRNA database (http://rrna.uia.ac.be). The sequences of our strains and the sequences of *Dientamoeba fragilis*, *Histomonas meleagridis*, *Trichomitopsis* and symbiont Im2 were appended to the alignment using ClustalX 1.81 (Thompson *et al.* 1997). The alignment was then manually refined in Bioedit sequence alignment editor (Hall, 1999). Alignments are available upon request.

Phylogenetic trees were constructed using maximum likelihood, maximum parsimony and neighbor-joining methods with LogDet distances in PAUP 4.0 beta 10 (Swofford, 1998) and by Bayesian methods in MrBayes3.1 (Ronquist and Huelsenbeck, 2003).

In MrBayes the base frequencies, rates for six different types of substitutions, number of invariant sites and shape parameter of the gamma correction for rate heterogeneity were allowed to vary, covarion was used to model the rate heterogeneity along the tree. 2000 000 generations of the Markov Chain Monte Carlo for the large analysis and 3 500 000 generations for the *Monocercomonas colubrorum* analysis were run with default settings (4 simultaneous chains, heating temperature 0.2). The first 2 000 trees for the large analysis and 15 000 trees for the *Monocercomonas colubrorum* analysis were removed as the "burn-in". In the *Monocercomonas colubrorum* analysis the data set was constructed by concatenating of SSU rDNA, ITS1, 5.8S rDNA, ITS2 and partial LSU rDNA and specific models with independent parameters were assigned to each gene.

Maximum likelihood trees were constructed in PhyML using the GTR+I+Γ model with parameters estimated by the software. Maximum parsimony and distance trees were constructed in PAUP4.0 (Swofford, 1998). For maximum parsimony tree construction, heuristic searching with ten replicates and random taxa addition was used. The neighbor-joining method with LogDet distances and estimated proportion of invariable sites was used to construct the distance trees. The proportions of invariable sites, 0.40 for the larger and 0.91 for the smaller analysis, were estimated in PAUP4.0. The node support was assessed by bootstrapping (100 replicates for maximum likelihood and 1000 replicates for maximum parsimony and distance methods).

ACKNOWLEDGEMENT

The authors would like to express thanks to Jana Bulantová for providing reptile material, Mirka Šedinová for sequencing, Jiří Zítek for programming the Grmeasure software, Joel B. Dacks and Alastair G. B. Simpson for reading the manuscript. The work was supported by the Czech Ministry of Education (project 0021620828), Czech Science Foundation (project 206/05/0371) and the Grant agency of Charles University (project 269/2004/B-Bio/PrF).

REFERENCES

Adl SM, Simpson AG, Farmer MA, Andersen RA, Anderson OR, Barta JR, Bowser SS, Brugerolle G, Fensome RA, Fredericq S, James TY, Karpov S, Kugrens P, Krug J, Lane CE, Lewis LA, Lodge J, Lynn DH, Mann DG, McCourt RM, Mendoza L, Moestrup O, Mozley-Standridge SE, Nerad TA, Shearer CA, Smirnov AV, Spiegel FW, Taylor MF (2005) The new higher level classification of eukaryotes with emphasis on the taxonomy of protists. J Eukaryot Microbiol **52:** 399-451.

Brugerolle G (1973) Sur l'existence de vrais kystes chez les Trichomonadines intestinales. Ultrastructure des kystes de *Trichomitus batrachorum* Perty 1852, *Trichomitus sanguisugae* Alexeieff 1911, et *Monocercomonas tipulae* Mackinnon 1910. C R Acad Sci Paris **277**: 2193-2196

Brugerolle G (1976) Cytologie ultrastructurale, systematique et evolution des Trichomonadida. Annales de la Station Biologique Besse-en-Chandesse **10**: 1-57

Brugerolle G (1991) Cell organization in free-living amitochondriate heterotrophic flagellates. In Patterson D and Larsen J (eds) The Biology of Free-living Heterotrophic Flagellates. Clarendon Press, Oxford, pp 133-148

Brugerolle G and Patterson PJ (2001) Ultrastructure of *Joenina pulchella* Grassi, 1917 (Protista, Parabasalia), a reassessment of evolutionary trends in the parabasalids, and a new order Cristamonadida for devescovinid, calonymphid and lophomonad flagellates. Org Divers Evol **1:**147-160

Clark CG and Diamond LS (2002) Methods for cultivation of luminal parasitic protists of clinical importance. Clin Microbiol Rev **15:** 329-341

Dacks JB and Redfield RJ (1998) Phylogenetic placement of Trichonympha. J Eukaryot Microbiol **45**: 445-447

Delgado-Viscogliosi P, Viscogliosi E, Gerbod D, Kulda J, Sogin ML, Edgcomb VP (2000) Molecular phylogeny of parabasalids based on small subunit rRNA sequences, with emphasis on the Trichomonadinae subfamily. J Eukaryot Microbiol **47**: 70-75

Dolan M, Wier AM, Melnitsky H, Whiteside JH, Margulis L (2004) Cysts and symbionts of *Staurojoenina assimilis* Kirby from *Neotermes*. Eur J Protistol **40**: 257-264

Edgcomb VP, Viscogliosi E, Simpson AGB, Delgado-Viscogliosi P, Roger AJ, Sogin ML (1998) New insights into the phylogeny of trichomonads inferred from small subunit rRNA sequences. Protist **149**:359-366

Farmer MA (1993). Ultrastructure of *Ditrichomonas honigbergii* n. g., n. sp. (Parabasalia) and its relationship to amitochondrial protists. J Eukaryot Microbiol **40**: 619-626

Felleisen RSJ (1997) Comparative sequence analysis of 5.8S rRNA genes and internal transcribed spacer (ITS) regions of trichomonadid protozoa. Parasitology **115**:111-119

Felsenstein J (1978) Cases in which parsimony or compatibility methods will be positively misleading. Syst Zool **27**:401-410

Gerbod D, Edgcomb VP, Noël C, Delgado-Viscogliosi P, Viscogliosi E (2000) Phylogenetic position of parabasalid symbionts from the termite *Calotermes flavicollis* based on small subunit rRNA sequences. Int Microbiol **3**:165-172

Gerbod D, Edgcomb VP, Noël C, Zenner L, Wintjens R, Delgado-Viscogliosi P, Holder ME, Sogin ML, Viscogliosi E (2001) Phylogenetic position of the trichomonad parasite of turkeys, *Histomonas meleagridis* (Smith) Tyzzer, inferred from small subunit rRNA sequence. J Euk Microbiol **48**:498-504

Gerbod D, Noël C, Dolan MF, Edgcomb VP, Kitade O, Noda S, Dufernez F, Ohkuma M, Kudo T, Capron M, Sogin ML, Viscogliosi E (2002) Molecular phylogeny of parabasalids inferred from small subunit rRNA sequences, with emphasis on the Devescovinidae and Calonymphidae (Trichomonadea). Mol Phylogenet Evol **25**:545-556

Gerbod D, Sanders E, Moriya S, Noël C, Takasu H, Fast NM, Delargo-Viscogliosi P, Ohkuma M, Kudo T, Capron M, Palmer JD, Keeling PJ, Viscogliosi E (2004) Molecular phylogenies of Parabasalia inferred from four protein genes and comparison with rRNA trees. Mol Phylogenet Evol **31**:572-580

Hall TA (1999) BioEdit: a user-friendly biological sequence alignment editor and analysis program for Windows 95/98/NT. Nucl Acids Symp Ser **41**: 95-98

Hampl V, Cepicka I, Flegr J, Tachezy J, Kulda J (2004) Critical analysis of the topology and rooting of the parabasalian 16S rRNA tree. Mol Phylogenet Evol **32**:711-723

Hampl V, Vrlík M, Cepicka I, Pecka Z, Kulda J, Tachezy J (2006) Affiliation of *Cochlosoma* to trichomonads confirmed by phylogenetic analysis of the small subunit rRNA gene and a new family concept of the order Trichomonadida. Int J Syst Evol Microbiol **56**: 305-312.

Hollande A and Caruette-Valentin J (1971) Les atractophores, l'induction du fuseau, et la division cellulaire chez les Hypermastigines, étude infrastructurale et révision systématique des Trichonymphines et des Spirotrichonymphines. Protistologica **7:**5-100

Honigberg BM (1955) Structure and morphogenesis of two new species of *Hexamastix* from lizards. J Parasitol **41**: 1-17

Honigberg BM (1963) Evolutionary and Systematic Relationships in the Flagellate Order Trichomonadida Kirby. J Protozool **10**: 20-63

Honigberg BM, Christian HH (1954) Characteristics of *Hexamastix batrachorum* (Alexeieff). J Parasitol **40**: 508-514

Jensen EA, Hammond DM (1964) A morphological study of trichomonads and related flagellates from the bovine digestive tract. J Protozool **11**: 386-394

Keeling PJ (2002) Molecular phylogenetic position of *Trichomitopsis termopsidis* (Parabasalia) and evidence for the Trichomitopsiinae. Eur J Protistol **38**: 279-286

Keeling PJ, Poulsen N, McFadden GI (1998) Phylogenetic diversity of parabasalian symbionts from termites, including the phylogenetic position of *Pseudotrypanosoma* and *Trichonympha*. J Euk Microbiol **45**: 643-650

Mattern CF, Honigberg BM, Daniel WA (1972) Structure of *Monocercomonas* sp. as revealed by electron microscopy. J Protozool **19**: 265-274

Moskowitz N (1951) Observations on some intestinal flagellates from reptilian host (Squamata). J Morphol **89**: 257-321

Nie D (1950) Morphology and taxonomy of the intestinal Protozoa of the guinea-pig, *Cavia porcella*. J Morphol **86**: 381-494

Noël C, Noda S, Mantini C, Dolan MF, Moriya S, Delargo-Viscogliosi P, Kudo T, Capron M, Pierce RJ, Ohkuma M, Viscogliosi E (2007) Molecular phylogenetic position of the genera *Stephanonympha* and *Caduceia* (Parabasalia) inferred from nuclear small subunit rRNA gene sequences. J Eukaryot Microbiol *in press*

Ohkuma M, Iida T, Ohtoko K, Yuzawa H, Noda S, Viscogliosi E, Kudo T (2005) Molecular phylogeny of parabasalids inferred from small subunit rRNA sequences, with emphasis on the Hypermastigea. Mol Phylogenet Evol **35**: 646-655

Ohkuma M, Ohtoko K, Grunau C, Moriya S, Kudo T (1998) Phylogenetic identification of the symbiotic hypermastigote *Trichonympha agilis* in the hindgut of the termite *Reticulitermes speratus* based on small-subunit rRNA sequence. J Eukaryot Microbiol **45**:439-444

Ohkuma M, Saita K, Inoue T, Kudo T (2006) Comparison of four protein phylogeny of parabasalian symbiontsin termite guts, doi:10.1016/j.ympev.2006.09.016

Ronquist F, Huelsenbeck JP (2003) MrBayes 3: Bayesian phylogenetic inference under mixed models. Bioinformatics **19**: 1572-1574

Swofford DL (1998) PAUP*. Phylogenetic Analysis Using Parsimony (*and Other Methods). Version 4. Sinauer Associates, Sunderland, Massachusetts

Tachezy J, Tachezy R, Hampl V, Sedinova M, Vanacova S, Vrlik M, Van Ranst M, Flegr J, Kulda J (2002) Cattle pathogen *Tritrichomonas foetus* (Riedmuller, 1928) and pig commensal *Tritrichomonas suis* (Gruby & Delafond, 1843) belong to the same species. J Euk Microbiol **49**: 154-163

Thompson JD, Gibson TJ, Plewniak F, Jeanmougin F, Higgins DG (1997) The ClustalX windows interface: flexible strategies for multiple sequence alignment aided by quality analysis tools. Nucleic Acids Res **24**: 4876-4882

Table 1. Information on the origin of strains included in the study. *Indicates that the host was examined in the wild or immediately after import to the Czech Republic.

Species	Strain	Host species	Isolation	GenBank number (SSU rDNA, ITS)
Monocercomonas colubrorum	R183	*Trophidophis melanurus**	Kulda (1966)	AY319276
Monocercomonas colubrorum	TSC	*Teratoscincus scincus*	Čepička (2000)	AY319277
Monocercomonas colubrorum	NS-1PRR (ATCC 50210)	*Natrix sipedon*	L.S. Diamond (1959)	AY319266, U17507
Monocercomonas colubrorum	R208	*Anolis equestris**	Kulda (1966)	AY319268
Monocercomonas colubrorum	PYR-1	*Python regius**	Kulda (1998)	AY319270
Monocercomonas colubrorum	EUMM	Eumeces sp.	Čepička (1999)	AY319278, AY319273
Monocercomonas colubrorum	HAD	*Ahaetula prasina**	Kulda (1994)	AY319267
Monocercomonas colubrorum	VAR-1	*Varanus exanthematicus**	Kulda (1998)	AY319272
Monocercomonas colubrorum	R186	*Trophidophis melanurus**	Kulda (1966)	DQ174302
Monocercomonas colubrorum	GRIS	*Varanus griseus**	Čepička (2004)	DQ174297
Monocercomonas colubrorum	LA10	*Lacerta agilis**	Kulda (1992)	DQ174300
Monocercomonas colubrorum	R293	Unidentified Cuban lizard	Kulda (1966)	DQ174303
Monocercomonas colubrorum	BIGA	Bitis gabonica*	Hampl (2004)	DQ174292
Monocercomonas colubrorum	MONT1	Chameleo montium*	Čepička (2004)	DQ174301
Monocercomonas colubrorum	CHEL1	Chameleo melleri*	Čepička (2004)	DQ174299
Monocercomonas colubrorum	HYDR1	Hydrosaurus pustullatus*	Čepička (2005)	DQ174298
Monocercomonas colubrorum	BOA5	Boa constrictor*	Čepička (2004)	DQ174295
Monocercomonas colubrorum	BOA1	Boa constrictor*	Čepička (2004)	DQ174293
Monocercomonas colubrorum	BOA4	Boa constrictor*	Hampl (2004)	DQ174294
Monocercomonas colubrorum	CORON1	Coronella austriaca*	Čepička (2005)	DQ174296
Honigbergiella ruminantium	KOJ-14	*Bos taurus*	Čepička (2000)	AY319280, AY319271
Honigbergiella ruminantium	HER-5	*Bos taurus*	Čepička (2000)	AY319279, AY319269
Hexamastix mitis	CYCL	*Cyclura nubila*	Čepička	AY319275
Hexamastix kirbyi	T	Uromastyx	Tachezy (1996)	AY321149
Honigbergiella sp.	ATCC 50321	*free-living*	Nerad (1987)	AY319274

Table 2. Dimensions (in μm) of protargol-stained specimens of *Monocercomonas colubrorum* strains. Average of 50 specimens±standard deviation (smallest-largest value). Representatives of clades are separated by a line.

Strain	Cell length	Cell width	Cell length/ cell width	Nucleus lenght	Nucleus width	Nucleus length/ nucleus width	Free portion of axostyle/ cell length
R183	***9.4±1.2 (7-12.2)***	4.1±0.6 (2-5.3)	2.3±0.5 (1.6-4.4)	2.1±0.4 (1.4-2.8)	1.3±0.2 (0.9-1.8)	1.6±0.3 (1-2.1)	0.4±0.2 (0.2-1)
R186	***9±1.2 (6.6-11.8)***	4.5±0.8 (2.2-6.1)	2.1±0.4 (1.3-3.6)	2±0.3 (1.3-2.7)	1.2±0.2 (0.8-1.6)	1.8±0.3 (1.2-2.7)	0.6±0.2 (0.3-1.2)
LA10	***9.7±1.3 (6.7-11.6)***	5.3±0.7 (4.1-6.6)	1.8±0.2 (1.3-2.3)	2.1±0.3 (1.6-2.9)	1.3±0.2 (0.8-1.8)	1.7±0.3 (1.3-2.5)	0.3±0.1 (0.2-0.6)
R293	8.8±1.0 (6.3-11.8)	4.6±0.5 (3.6-5.8)	1.9±0.2 (1.4-2.4)	2±0.3 (1.4-2.8)	1.2±0.2 (0.7-1.7)	1.7±0.4 (1.2-3.9)	0.3±0.1 (0.2-0.5)
TSC	***9.5±1.1 (6.8-12)***	6.2±0.8 (4.6-7.6)	1.6±0.2 (1.1-2.2)	2.2±0.4 (1.2-3.5)	1.3±0.3 (0.8-2.1)	1.8±0.3 (1.2-2.5)	0.3± 0.1 (0.1-0.5)
NS-1PRR	***8.2±0.8 (6.5-10)***	4.2±0.4 (3.5-4.9)	2±0.2 (1.6-2.4)	2.1±0.2 (1.5-2.5)	1.2±0.2 (0.8-1.6)	1.8±0.3 (1.3-2.8)	0.3±0.1 (0.1-0.4)
EUMM	11.4±1.4 (8.8-15.2)	5.6±0.9 (4.1-8.5)	2.1±0.3 (1.3-3.1)	2.3±0.3 (1.8-3.8)	1.2±0.2 (0.9-2.7)	2±0.3 (1.4-2.7)	0.5±0.2 (02-0.9)
HAD	9.4±0.8 (7.4-11.3)	4.2±0.4 (3.1-5)	2.3±0.3 (1.7-2.9)	2.2±0.3 (1.7-2.7)	1.2±0.2 (0.9-1.7)	1.8±0.3 (1.3-2.5)	0.4±0.1 (0.2-0.5)
HYDR1	9,5±0.8 (7.5-12.2)	4,3±0.4 (3.3-5.7)	2,2±0.2 (1.8-3)	2,2±0.3 (1.7-2.8)	1,3±0.1 (1-1.7)	1,7±0.2 (1.2-2.4)	0,3±0.1 (0.1-0.4)
BOA5	9.3±1.0 (7.1-12)	4.3±0.4 (3.6-5.3)	2.2±0.2 (1.7-2.7)	2±0.3 (1.3-2.7)	1.2±0.2 (0.9-2.1)	1.7±0.3 (1.3-2.4)	0.3±0.1 (0.1-0.4)

Table 3. Summary of morphological characters for species studied in this paper and families of Trichomonadida. (Um – undulating membrane, Ib – infrakinetosomal body, Co – comb-like structure, ML – marginal lamella, + character present, - character absent)

	Trunk of axostyle	Capitulum of axostyle	Pelta	Parabasal body	Um	Ib	Co	ML	Costa
Honigbergiella ruminantium	Slender	Narrow	Small	Disc with dark central granule	-	-	-	-	-
Honigbergiella sp.	Slender	Narrow	Small	Disc with dark central granule	-	-	-	-	-
Hexamastix mitis	Slender	Narrow	Small	Disc with dark central granule	-	-	-	-	-
Hexamastix kirbyi	Slender	Scoop-like, abruptly widening	Large, wavy	Tear or ring with dark outline	-	-	-	-	-
Monocercomonas colubrorum	Stout, tapering continuously to the tip	Spoon-like, slowly widening	Large, scoop-like	Rod	-	+	+	+	-
Trichomonadidae	Slender	Various	Various	Various	Lameliform	-	-	–	Type B
Tritrichomonadidae	Stout, with short projection tapering abruptly to the conical tip	Spoon like, slowly widening	Small , crescent-shaped	Rod	Railform	+	+	+	Type A
Trichomitidae	Moderate diameter, long gradually tapering projection	Spatulate or spoon-shaped with lateral extensions, slowly widening	Large, crescent-shaped	Biramous	Lameliform	-	+	+	Type A

FIGURE LEGENDS

Figure 1: Polyphyly of Monocercomonadidae. Unrooted phylogenetic tree of parabasalids based on SSU rDNA sequences, constructed by maximum likelihood method. The values at the nodes indicate statistical support estimated by four methods (distance bootstrap/MP bootstrap/ML bootstrap/MrBayes posterior probability). GenBank accession numbers are supplied for the termite-symbiont sequences. Shaded boxes indicate orders Trichonymphida, Spirotrichonymphida and Cristamonadida; species outside the boxes belong to the order Trichomonadida. Families of Trichomonadida according to Hampl *et al.*. (2006) are indicated. Asterices indicate that the node was not recovered by a particular method.

Figure 2: Phylogenetic tree of *Monocercomonas colubrorum* strains based on concatenated SSU rDNA and ITS region (5.8S rDNA, ITS1, ITS2 and partial 28S rDNA) sequences. The tree was constructed by the maximum likelihood method and rooted on clade 1. The values at the nodes indicate statistical support estimated by four methods (distance bootstrap/maximum parsimony bootstrap/maximum likelihood bootstrap/Bayesian posterior probabilities). The hosts group (S-snake, L-lizard) is indicated for each strain. The tree was rooted on clade 1. The basal position of this clade was recovered (bootstrap support 94% and above) in separate analyses using *Tritrichomonas foetus* as an outgroup. Asterices indicate that the node was not recovered by particular method.

Figure 3: Protargol stained specimens of *Honigbergiella ruminantium* strain HER-5 (A, B) and *Honigbergiella sp*. strain ATCC 50321 (C, D). Arrows indicate the parabasal body, bars = 10μm.

Figure 4: Line drawings of *Honigbergiella ruminantium* strain HER-5 (A) and *Honigbergiella sp*. strain ATCC 50321 (B). Ax – axostyle, Pb – parabasal body, Pe – pelta, Pf – parabasal fiber.

Figure 5: Ultrastructure of *Honigbergiella ruminantium* strain HER-5. A-C, mastigont of trophozoite; D, cyst. 1, 2, 3, R – basal bodies, Ax – axostyle, Cv – cyst wall, Fv – food vacuole, Gb – Golgi body, Gl – glycocalyx, H – hydrogenosome, Ifl – internalized flagellum, N – nucleus, Pe – pelta, Pf – parabasal fiber.

Figure 6: Ultrastructure of *Honigbergiella* sp. strain ATCC 50321. A-C, mastigont of trophozoite; D, cyst. 1, 2, 3, R – basal bodies, Ax – axostyle, Cv – cyst wall, Gb – Golgi body, Gl – glycocalyx, H – hydrogenosome, N – nucleus, Pe – pelta, Pf – parabasal fiber, Rfl – recurrent flagellum, F2 – sigmoid fiber.

Figure 7: Protargol stained specimens of *Monocercomonas colubrorum* strains, arrow indicates the parabasal body, bars = 10μm. A - La10; B - NS1-PR; C – BOA5; D –R183.

Figure 8: Ultrastructure of *Monocercomonas colubrorum* strain VAR1. A, longitudinal section of a trophozoite with mastigont; B, transversal section of trophozoite; C, pseudocyst. 1, 2, 3, R – basal bodies, Ax – axostyle, Co – comb-like structure, Gb – Golgi body, H – hydrogenosome, Ib – infrakinetosomal body, Ifl – internalized flagellum, N – nucleus, Ml – marginal lamella, Pe – pelta, Pf – parabasal fiber, F2 – sigmoid fiber.

Figure 9: Protargol stained specimens of *Hexamastix mitis* strain CYCL (A-D) and *Hexamastix kirbyi* strain T (E-H), bars = 10μm (in A, B, C, G, H) and 5μm (in D, E, F). Ax – expanded capitulum of axostyle, Pb – parabasal body, Pe – pelta.

Figure 10: Line drawings of *Hexamastix mitis* strain CYCL (A, B) and *Hexamastix kirbyi* strain T (C, D). Ax – axostyle, Pb – parabasal body, Pe – pelta, Pf – parabasal fiber.

Figure 11: Ultrastructure of *Hexamastix kirbyi* strain T. A-D, mastigont. 1, 2, 3, 4, 5 – basal bodies, Ax – axostyle, F1, F2 – sigmoid fibers, F3 – hooked lamina, Gb – Golgi body, N – nucleus, Pe – pelta, Pf – parabasal fiber, Rfl – recurrent flagellum.

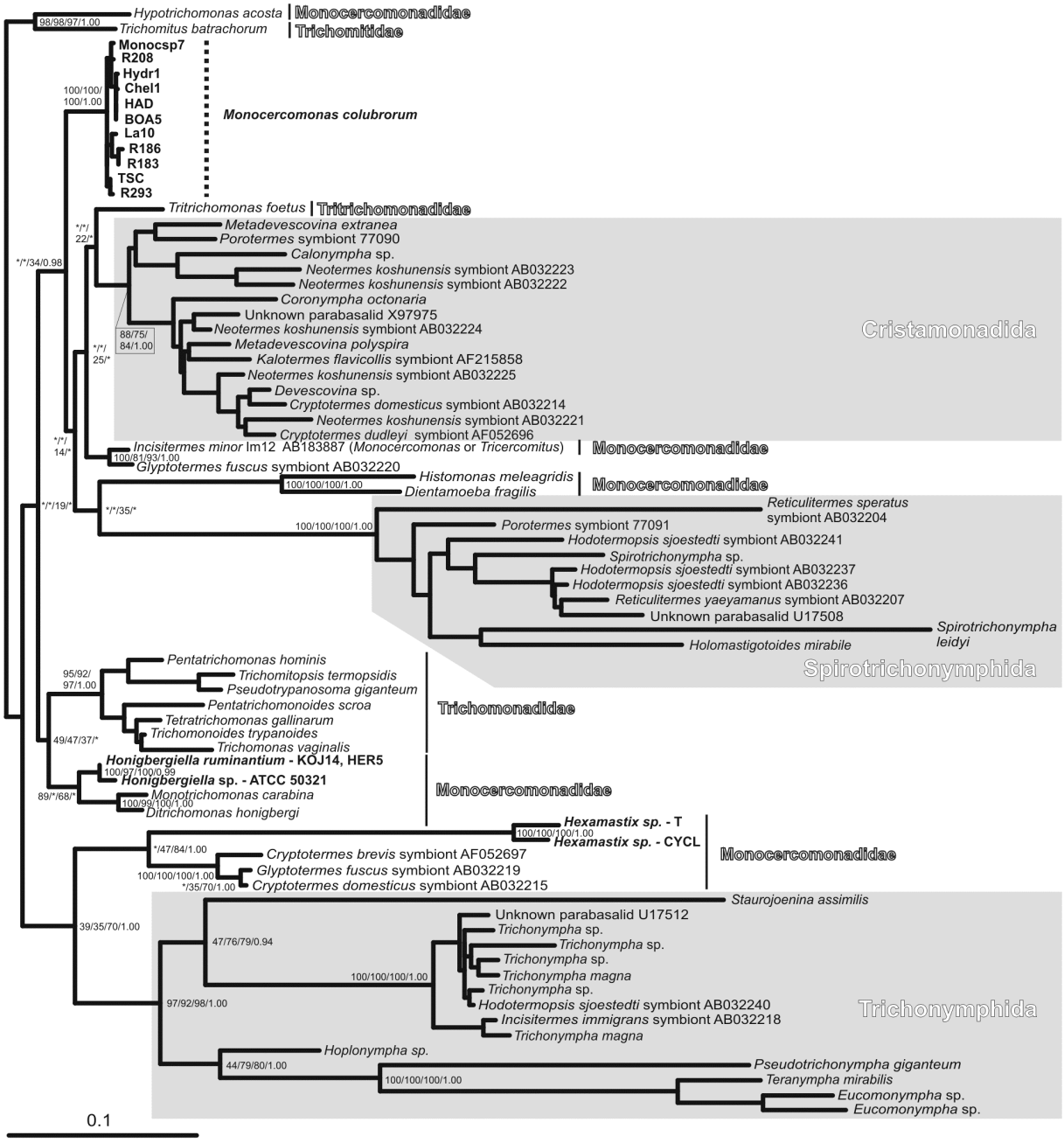
Hypotrichomonas acosta
Trichomitus batrachorum
Monocercomonadidae
Trichomitidae
98/98/97/1.00
Monocsp7
R208
Hydr1
Chel1
HAD
BOA5
La10
R186
R183
TSC
R293
100/100/
100/1.00
Monocercomonas colubrorum
Tritrichomonas foetus
Tritrichomonadidae
Metadevescovina extranea
Porotermes symbiont 77090
Calonympha sp.
Neotermes koshunensis symbiont AB032223
Neotermes koshunensis symbiont AB032222
Coronympha octonaria
Unknown parabasalid X97975
Neotermes koshunensis symbiont AB032224
Metadevescovina polyspira
Kalotermes flavicollis symbiont AF215858
Neotermes koshunensis symbiont AB032225
Devescovina sp.
Cryptotermes domesticus symbiont AB032214
Neotermes koshunensis symbiont AB032221
Cryptotermes dudleyi symbiont AF052696
Cristamonadida
//34/0.98
//
22/*
88/75/
84/1.00
//
25/*
//
14/*
Incisitermes minor lm12 AB183887 (Monocercomonas or Tricercomitus)
Monocercomonadidae
100/81/93/1.00
Glyptotermes fuscus symbiont AB032220
Histomonas meleagridis
100/100/100/1.00
Dientamoeba fragilis
Monocercomonadidae
//19/*
//35/*
Reticulitermes speratus
symbiont AB032204
100/100/100/1.00
Porotermes symbiont 77091
Hodotermopsis sjoestedti symbiont AB032241
Spirotrichonympha sp.
Hodotermopsis sjoestedti symbiont AB032237
Hodotermopsis sjoestedti symbiont AB032236
Reticulitermes yaeyamanus symbiont AB032207
Unknown parabasalid U17508
Spirotrichonympha leidyi
Holomastigotoides mirabile
Spirotrichonymphida
Pentatrichomonas hominis
95/92/
97/1.00
Trichomitopsis termopsidis
Pseudotrypanosoma giganteum
Pentatrichomonoides scroa
Tetratrichomonas gallinarum
Trichomonoides trypanoides
49/47/37/*
Trichomonas vaginalis
Trichomonadidae
Honigbergiella ruminantium - KOJ14, HER5
100/97/100/0.99
Honigbergiella sp. - ATCC 50321
89/*/68/*
Monotrichomonas carabina
100/99/100/1.00
Ditrichomonas honigbergi
Monocercomonadidae
Hexamastix sp. - T
100/100/100/1.00
Hexamastix sp. - CYCL
Monocercomonadidae
*/47/84/1.00
Cryptotermes brevis symbiont AF052697
100/100/100/1.00
Glyptotermes fuscus symbiont AB032219
*/35/70/1.00
Cryptotermes domesticus symbiont AB032215
Staurojoenina assimilis
39/35/70/1.00
47/76/79/0.94
Unknown parabasalid U17512
Trichonympha sp.
Trichonympha sp.
Trichonympha sp.
100/100/100/1.00
Trichonympha magna
Trichonympha sp.
97/92/98/1.00
Hodotermopsis sjoestedti symbiont AB032240
Incisitermes immigrans symbiont AB032218
Trichonympha magna
Trichonymphida
Hoplonympha sp.
44/79/80/1.00
Pseudotrichonympha giganteum
100/100/100/1.00
Teranympha mirabilis
Eucomonympha sp.
Eucomonympha sp.
0.1

Figure 1

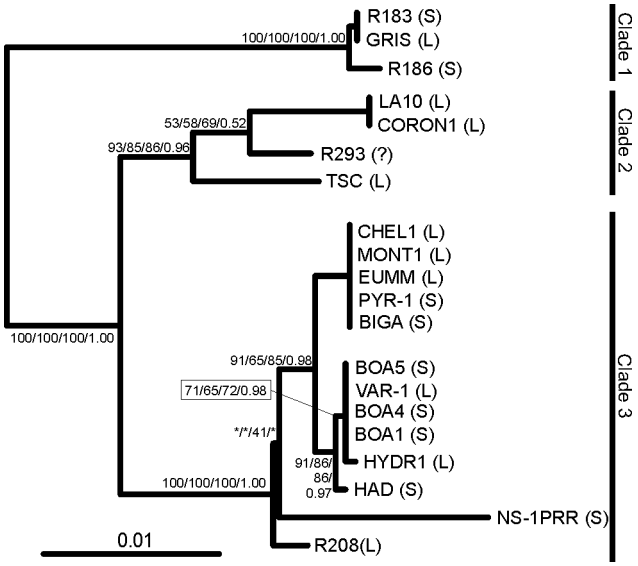

Figure 2

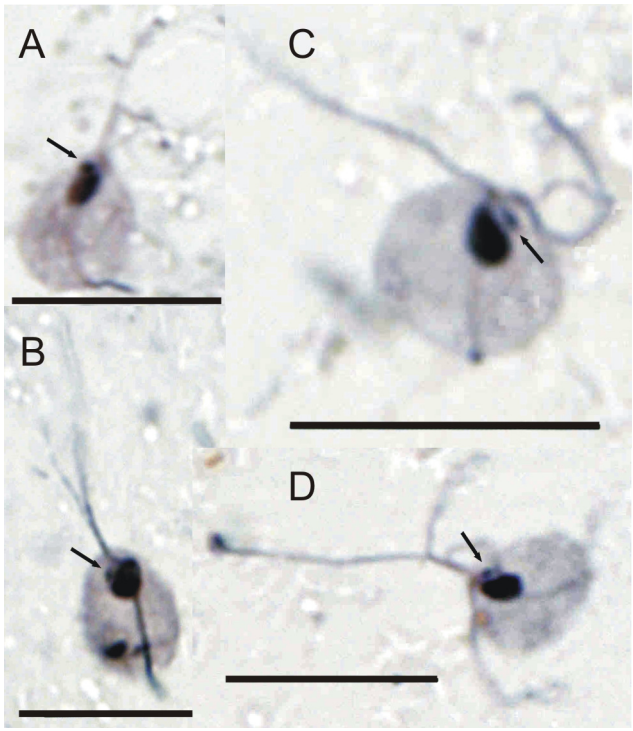

Figure 3

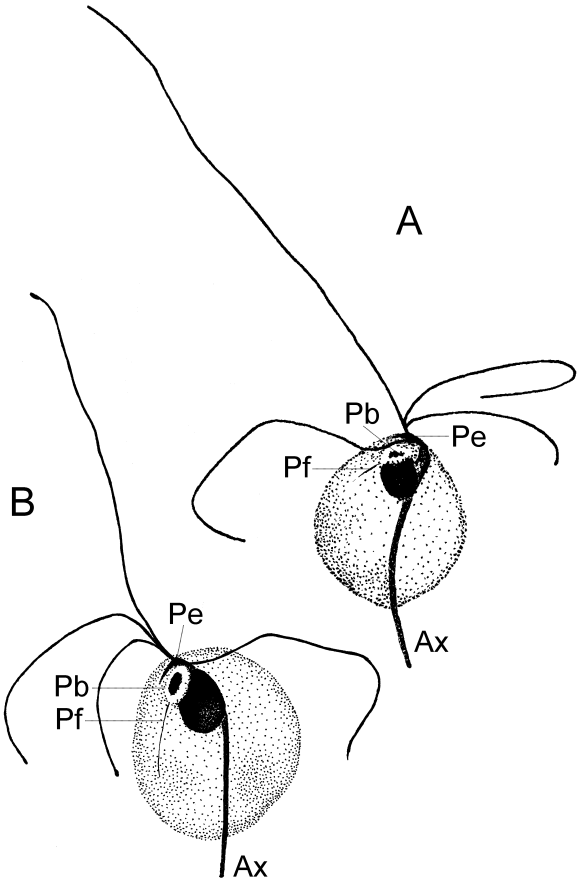

Figure 4

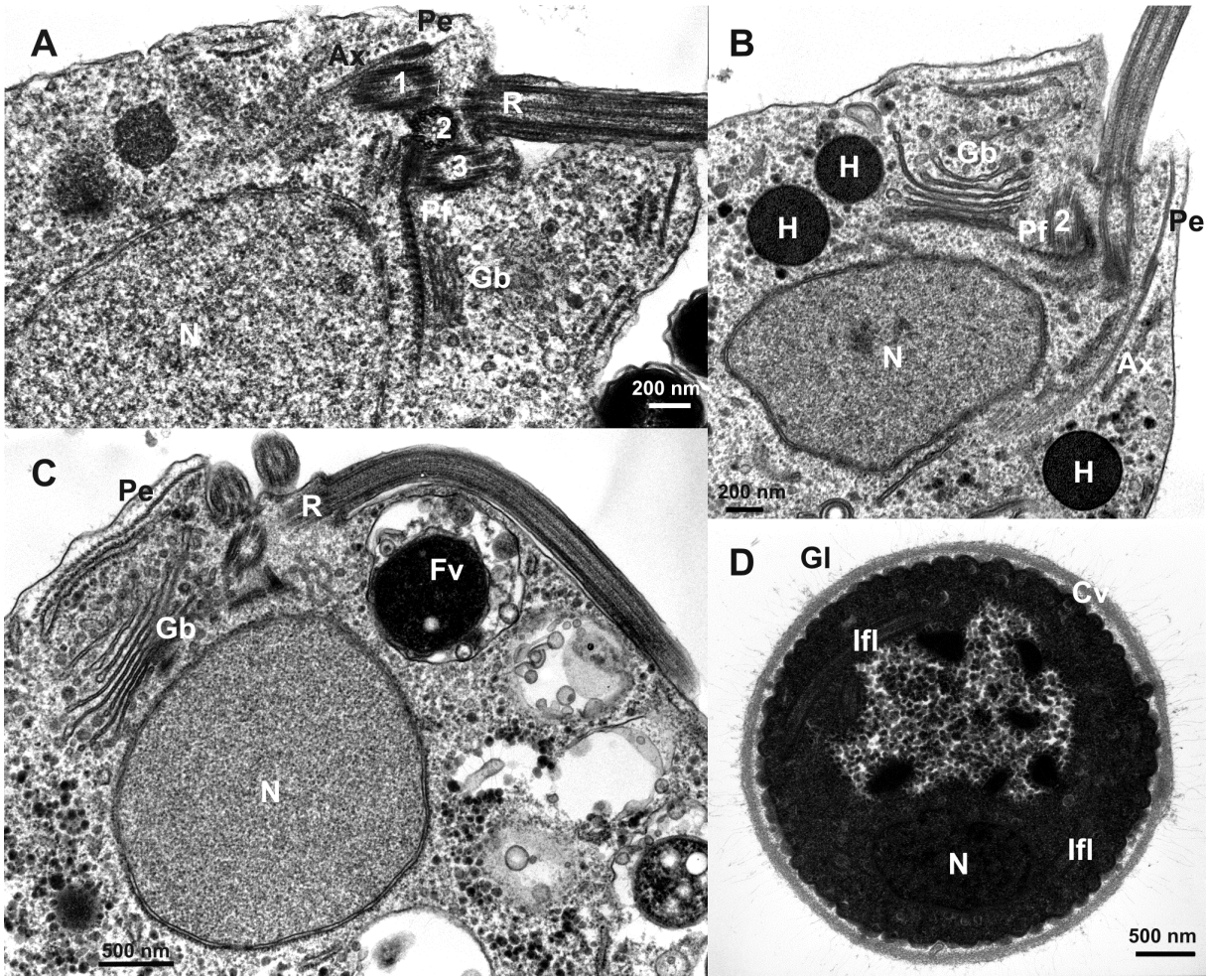
A
Pe
Ax
1
2
3
R
Pf
Gb
N
200 nm
B
H
H
Gb
Pf
2
Pe
N
Ax
H
200 nm
C
Pe
R
Fv
Gb
N
500 nm
D
Gl
Cv
Ifl
N
Ifl
500 nm

Figure 5

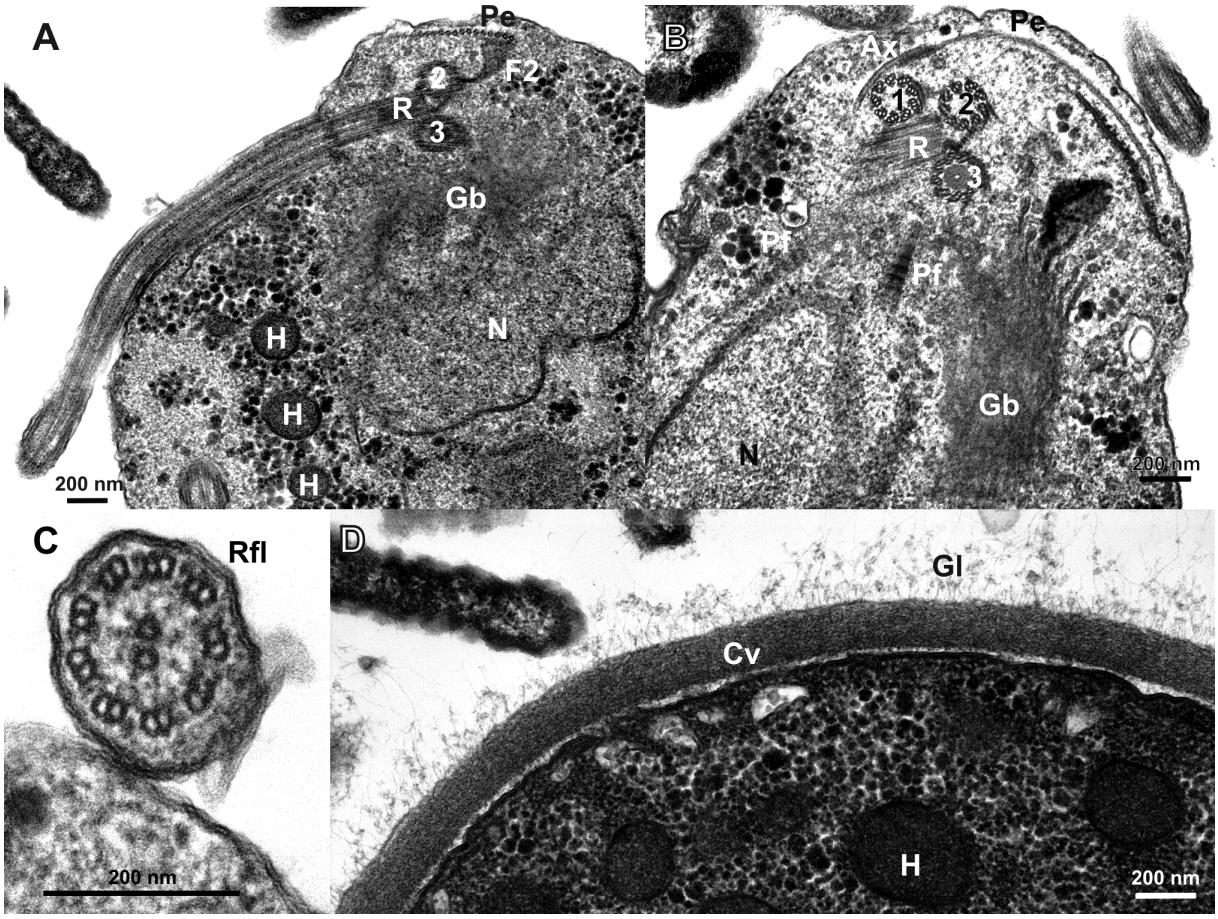
A
Pe
F2
2
R
3
Gb
H
N
H
H
200 nm
B
Ax
Pe
1
2
R
3
Pf
Pf
Gb
N
200 nm
C
Rfl
200 nm
D
Gl
Cv
H
200 nm

Figure 6

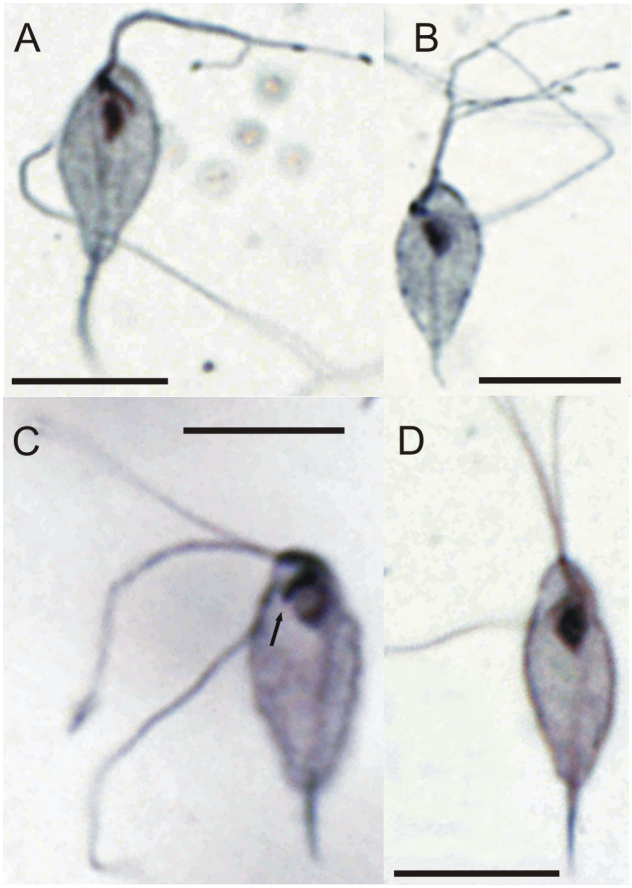

Figure 7

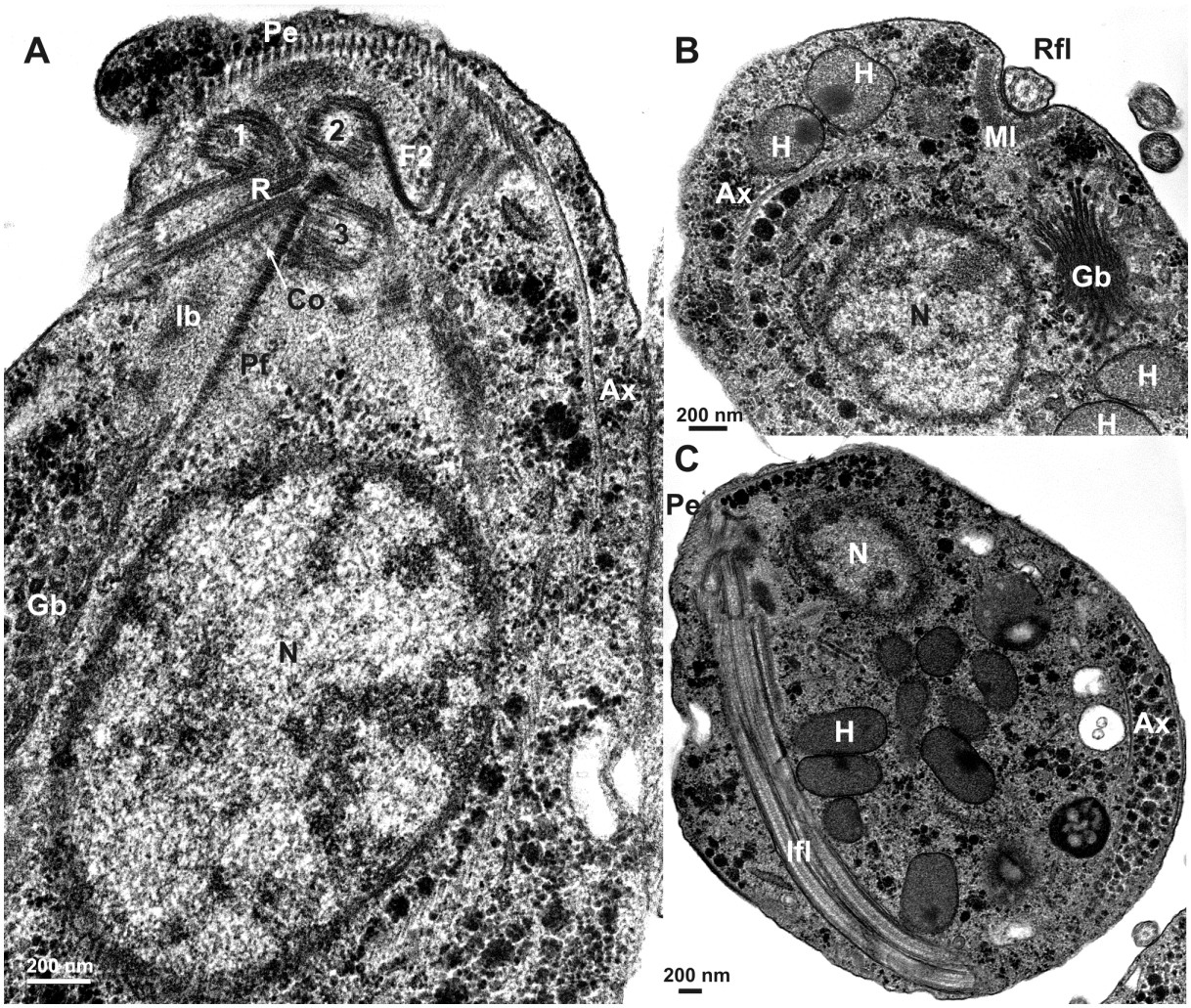
A
Pe
1
2
F?
R
3
Co
Ib
Pf
Ax
Gb
N
200 nm
B
Rfl
H
H
Ml
Ax
Gb
N
H
H
200 nm
C
Pe
N
H
Ax
Ifl
200 nm

Figure 8

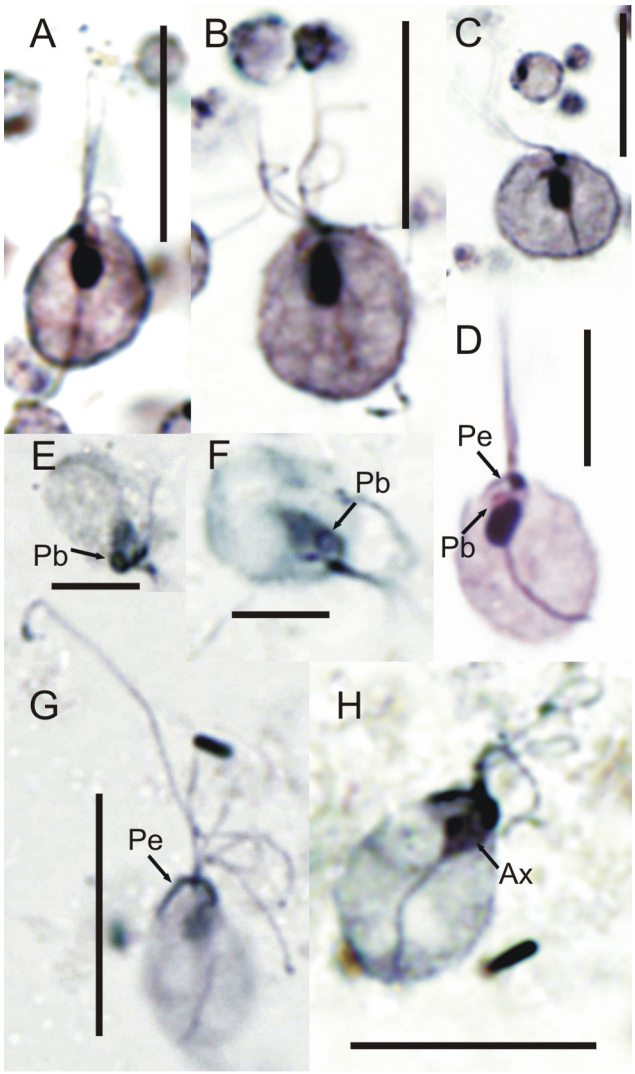

Figure 9

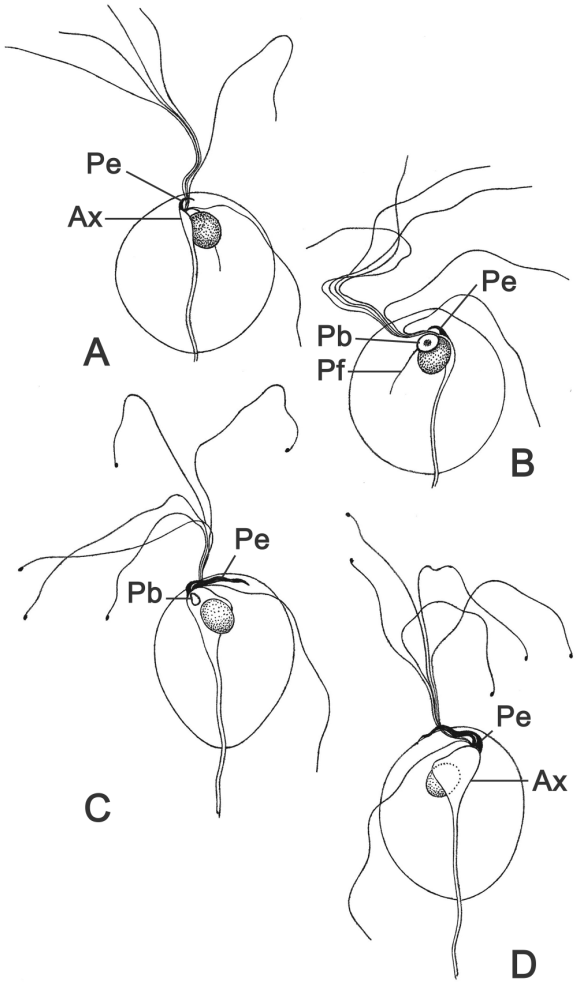

Figure 10

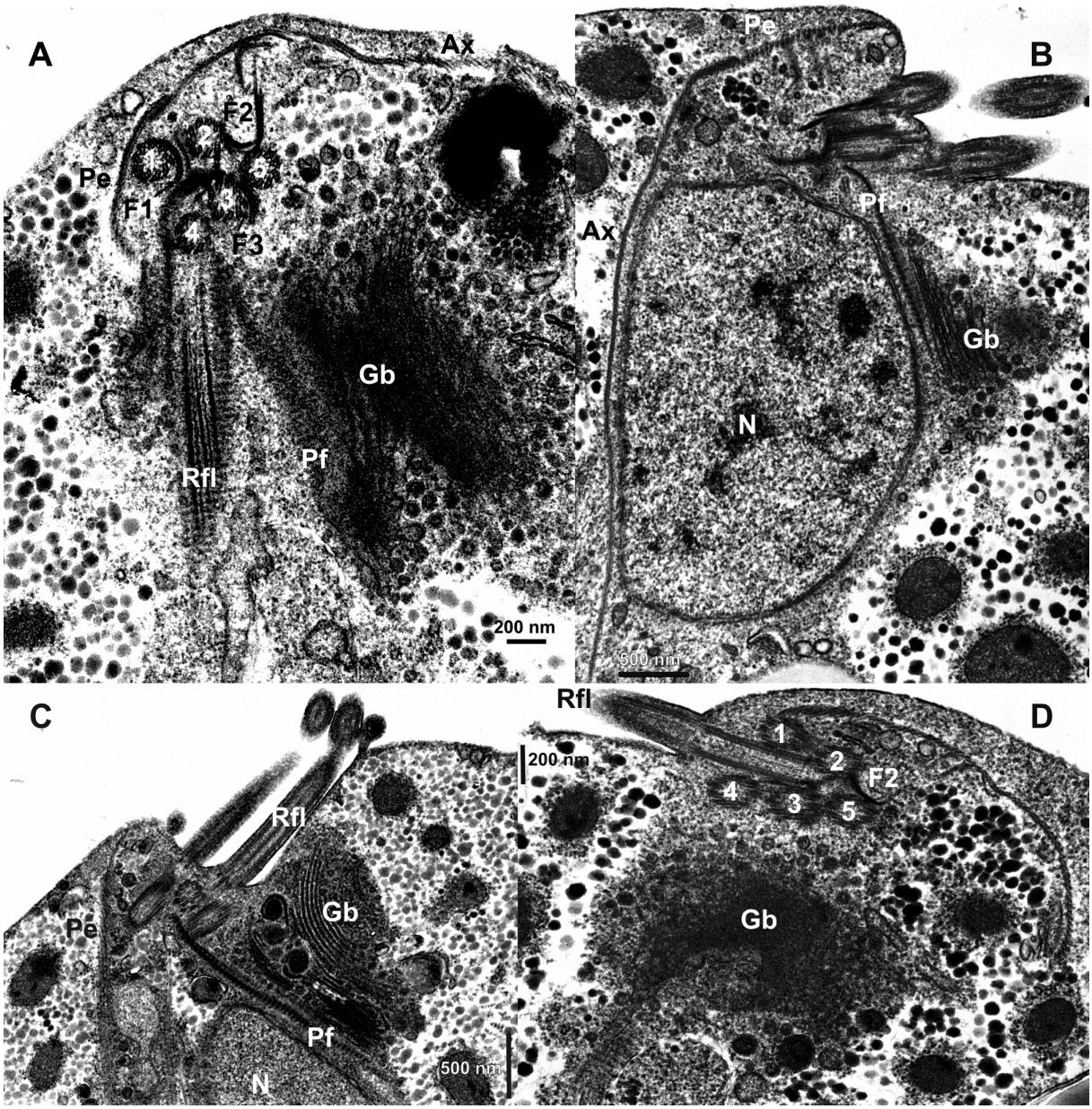
A
Ax
F2
2
5
Pe
F1
1
3
4
F3
Gb
Rfl
Pf
200 nm
B
Pe
Pf
Ax
Gb
N
500 nm
C
Rfl
200 nm
Rfl
Gb
Pe
Pf
N
500 nm
D
1
2
F2
4
3
5
Gb

Figure 11